

Interaction of Pt and Rh nanoparticles with ceria supports: Ring opening of methylcyclobutane and CO hydrogenation after reduction at 373–723 K

M. Fuchs^{a,1}, B. Jenewein^a, S. Penner^a, K. Hayek^{a,*}, G. Rupprechter^b,
D. Wang^b, R. Schlögl^b, J.J. Calvino^c, S. Bernal^c

^a *Institut für Physikalische Chemie, Leopold-Franzens-Universität, Innsrain 52A, A-6020 Innsbruck, Austria*

^b *Fritz-Haber-Institut der Max-Planck-Gesellschaft, Faradayweg 4-6, D-14195 Berlin, Germany*

^c *Departamento de Ciencia de los Materiales e Ingeniería Metalúrgica y Química Inorgánica, Universidad de Cádiz, Apartado 40, Puerto Real, E-11510 Cádiz, Spain*

Received 17 May 2005; received in revised form 21 July 2005; accepted 25 July 2005

Abstract

The catalytic properties of a Pt (4%) and a Rh (2.5%) catalyst on a low-surface area ceria support were determined as a function of hydrogen reduction in the temperature range between 373 and 723 K and compared to those of silica-supported Rh (3%) subjected to equivalent treatments. Two reactions were studied: the ring opening of methylcyclobutane (MCB) as representative for structure-sensitive hydrocarbon reactions and the hydrogenation of CO as an example for C–O bond activation. After reduction in the low- and mid-temperature range the rates of either reaction decrease significantly on ceria-supported Pt and Rh whereas they are hardly affected on Rh–silica. Annealing in vacuum at 723 K before the reduction step has a beneficial effect on the reaction rates but annealing after reduction leads to a general activity decrease. Accompanying *ex situ* high-resolution electron microscopy (HREM) investigations largely exclude particle decoration and formation of noble metal–Ce intermetallic bonds as possible effects of metal–support interaction at low and medium reduction temperatures. Taking also into account parallel surface science studies it is concluded that the observed activity decrease originates mainly from electronic perturbations at the interface between the metal nanoparticles and the increasingly reduced ceria support.

© 2005 Elsevier B.V. All rights reserved.

Keywords: Platinum; Rhodium; Ceria; Silica; Hydrogen reduction; Electron microscopy; Alloy formation; Methylcyclobutane; CO hydrogenation

1. Introduction

Ceria-supported platinum and rhodium are important catalysts for deNO_x and combustion reactions. Reducible oxide supports like ceria generally enhance the catalytic activity of the metal, but the catalysts are sensitive to hydrogen reduction at elevated temperature which may cause altered chemisorptive and catalytic properties, structural changes and catalyst deactivation. Strong metal–support interaction (SMSI [1]) between noble metal particles and a reducible support

under reduction in hydrogen has been under discussion for many years. Decoration of free metal surface by moieties of reduced support and inherent electronic perturbations very likely account for most SMSI phenomena observed on titania-supported [2–7] and vanadia-supported [8] noble metal particles. Decoration may be reversed upon exposure to oxygen or air [4,5,9].

On the other hand, hydrogen reduction of cerium oxide supports at 873 K and above leads to different oxides of type Ce_nO_{2n–2m}. So far, *ex situ* electron microscopy studies have revealed metal particle decoration after hydrogen treatment at 973 K and above [10–13]. Nevertheless, chemisorption data and catalytic measurements indicate appreciable interaction between ceria and noble metals already after

* Corresponding author. Tel.: +43 512 507 5062; fax: +43 512 507 2925.

E-mail address: konrad.hayek@uibk.ac.at (K. Hayek).

¹ Present address: Infineon Technologies, A-9500 Villach, Austria.

reduction at 773 K and below [12,14–16]. If decoration of the metal surface by mobile oxide species is a priori excluded, the altered catalytic properties must be either due to electronic effects associated to the increasing reduction of the ceria surface, or to an incipient formation of noble metal–cerium alloys.

While most studies in the past have been concerned with reduction at 773 K and above, the present work emphasizes the influence of hydrogen reduction on the catalytic behaviour of well-characterized Pt/CeO₂ and Rh/CeO₂ catalysts at low and medium temperature [LTR (373–523 K), resp. MTR (573–723 K)] and the results are analyzed with respect to possible mechanisms of metal-oxide interaction. An Rh/SiO₂ catalyst is studied in parallel as representative for metal phases dispersed on less-reducible supports. Two standard reactions are monitored: the hydrogenolysis (ring opening) of methylcyclobutane (MCB) and the hydrogenation of carbon monoxide. It is well known that CO hydrogenation is favoured by addition of reducible oxides to noble metal catalysts [17]. After high-temperature reduction the reaction rate on Rh/ceria may be enhanced under transient conditions [18].

The hydrogenolysis of MCB, on the other hand, is an example for skeletal hydrocarbon transformations, a type of processes well known as SMSI-sensitive. It occurs easily at 373 K and below and is therefore suited to quantify the effect of reduction in the low- and mid-temperature range. At low temperature and in hydrogen excess only the ring opening products (*n*-pentane and isopentane) are formed, but reaction rate and product distribution are structure-sensitive [19,20] and also strongly hydrogen pressure-dependent [20–22]. While the sterically less hindered isopentane formation predominates on Ni [21] and on Rh [21,23], statistical ring opening may occur on Pt [20,22] and Pd [21] catalysts. The pathway to statistical ring opening is most likely connected to the ability to form a flat-lying intermediate, which in turn is determined by structural properties, e.g. facet size and metal-support interface [24]. Its occurrence depends on the hydrogen pressure [21,22], the particle size [20] and the temperature.

Finally, high-resolution electron microscopy (HREM) was used to provide information about possible alloy formation due to reduction at higher temperature. The discussion of the reported results will also take into account some recent information obtained on “inverse” CeO_x/Rh systems [25] and on “thin film” noble metal/CeO_x catalysts [26].

2. Experimental

2.1. Catalyst preparation and characterization

The Pt (4%)/CeO₂ and the Rh (2.5%)/CeO₂ catalyst used in these experiments were in part characterized in a previous high-resolution electron microscopy study [12], and their

metal dispersion and morphology were therefore well known. In order to avoid the effect of chlorine on the structural and redox properties of ceria [27–29] they were prepared by incipient wetness impregnation from aqueous solutions of chlorine-free precursors, [Pt(NH₃)₄](OH)₂ and Rh(NO₃)₃. The support was low-surface area (4 m² g⁻¹) commercial ceria (99.9% pure), from Alpha. After impregnation, both catalysts were dried, calcined and reduced at 773 K. From [12] it is known that the increase of reduction temperature up to 773 K induces moderate metal sintering, whereby the metal dispersion of the Pt/CeO₂ catalyst decreases from 50 to 40%, and that of the Rh/CeO₂ sample from 46 to 38%, while the mean particle sizes both increase from about 2.5 to 3.5 nm.

An Rh (3%)/silica catalyst with Rh particles of comparable size was prepared and treated in the same way as the ceria-supported catalysts mentioned above. A SiO₂ Cabosil M-5 sample with a BET surface area of 190 m² g⁻¹ was impregnated with an aqueous solution of Rh(NO₃)₃, and further dried, calcined, and reduced at 773 K. As revealed by HREM and chemisorption measurements, this procedure resulted in a similar metal dispersion and mean particle size of the resulting catalyst (44% and about 3 nm, respectively, as also shown previously [30]).

Finally, for an EM study of the effect of high-temperature reduction on a less-reducible support, a Pt/SiO₂ catalyst of high metal loading (20%) was prepared from the precursor described above. It was calcined and reduced at 673 K and thereafter treated in 1 bar hydrogen under exactly the same conditions as the other catalysts and also as the corresponding thin film model system [31].

The catalysts were characterized by electron microscopy and microdiffraction in a Zeiss EM 10C, a Philips CM 200 FEG and a JEOL 2000 EX.

2.2. Catalytic reactions

Initially, all catalysts were subjected to redox cycles consisting of heating in 1 bar oxygen at 673 K for 2 h, followed by reduction in 1 bar hydrogen at 523 K until they reached a constant and reproducible activity. At the end, and also after every reaction, a standard oxidative treatment (1 bar O₂ at 673 K for 120 min) was applied, sufficient to reverse metal–ceria interaction effects of purely electronic origin [12,16]. The catalyst samples were then reduced in 1 bar hydrogen for 60 min at variable temperature before being exposed to the reactants in a computer-controlled microreactor of the recirculation type [32]. Furthermore, in some experiments annealing in vacuum (at 723 K for 30 min) was included before or after the reduction step. The reactant pressures under standard reaction conditions were 10 mbar hydrocarbon and 100 mbar hydrogen for MCB hydrogenolysis and 10 mbar CO and 100 mbar H₂ for CO hydrogenation, always with He added to 1 bar total pressure. From the conversion versus time plots, initial reaction rates were determined as a function of reactant partial pressures,

reaction temperature and temperature of hydrogen pretreatment. The turnover frequencies (TOF) were usually related to the metal surface area in the pristine state, i.e. to the initial dispersion determined by electron microscopy, but corrections were applied when particle sintering was known to occur.

3. Results

3.1. Evidence by electron microscopy

3.1.1. The Pt (4%)/CeO₂ and the Rh (2.5%)/CeO₂ catalyst after reduction

Fig. 1 shows profile view images of the Pt (4%)/CeO₂ catalyst after reduction at 473 K (a), 623 K (b), and 773 K (c), while Fig. 2 is representative for the Rh (2.5%)/CeO₂

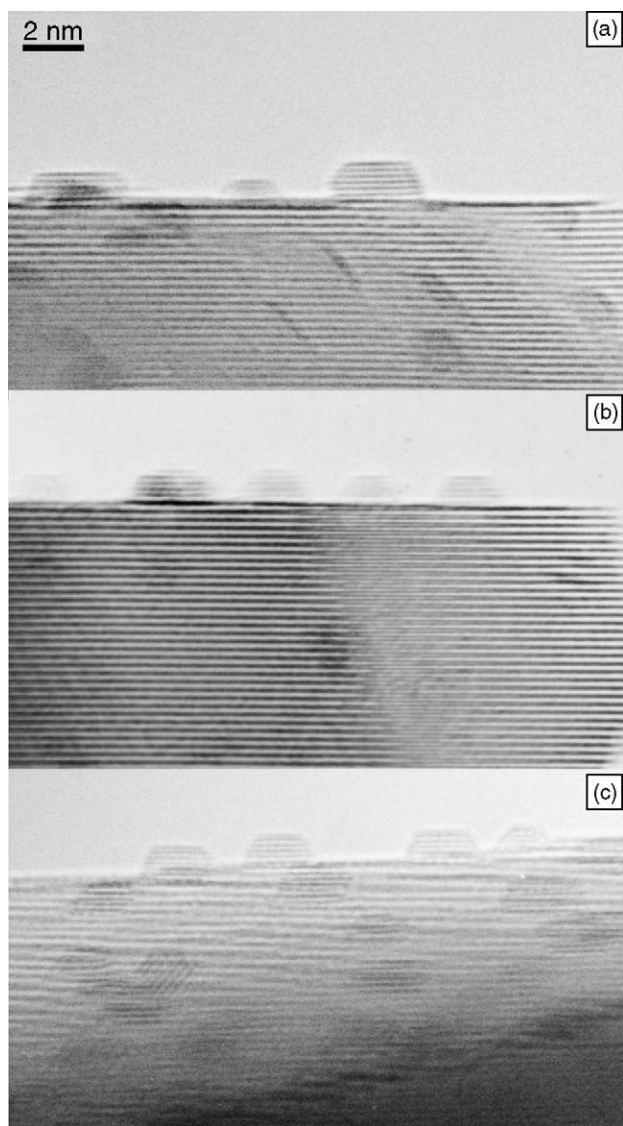


Fig. 1. The Pt (4%)/CeO₂ catalyst reduced at 473 K (a); 623 K (b); and 773 K (c).

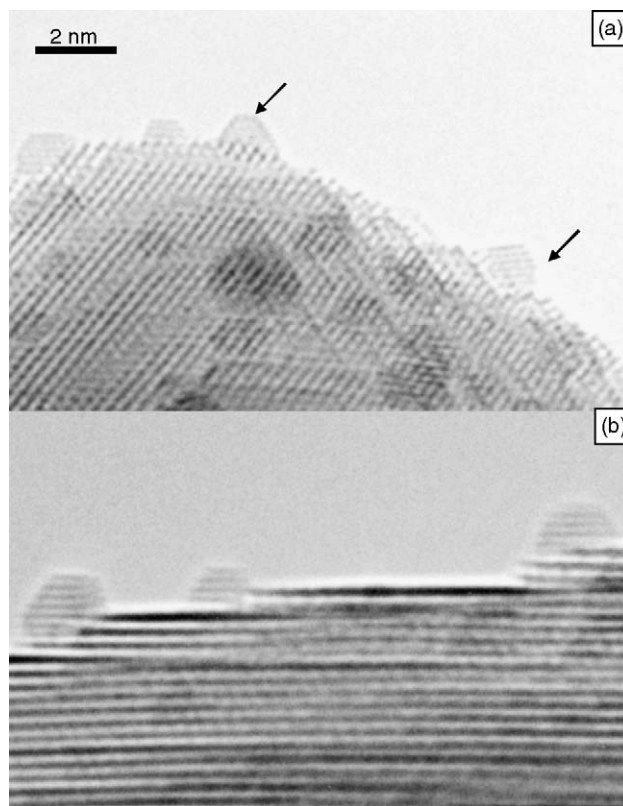


Fig. 2. The Rh (2.5%)/CeO₂ catalyst reduced at 623 K (a) and 773 K (b). The arrows in (a) indicate “disordered” particles.

catalyst after reduction at 623 K (a) and 773 K (b). It should be noted that the images were taken ex situ and hence may not be representative for the particle surface under working conditions of the catalyst. However, no HREM evidence of *irreversible* metal decoration or alloying could be detected on either catalyst in the studied range of reduction temperatures (473–773 K). While the Pt particles on top of the ceria support (Fig. 1) appear unchanged after hydrogen treatment up to 773 K, signs of slight surface disorder are recognized on some of the rhodium particles after reduction at 623 K (e.g. Fig. 2a, arrow), but not after reduction at 773 K (Fig. 2b). On the other hand, it appears that with increasing reduction temperature more and more metal particles are anchored at defect sites of the support, e.g. at newly formed step edges, as will be also discussed in Section 4.

3.1.2. Influence of hydrogen reduction on the mobility of crystalline ceria

Although the low-surface ceria used in this study shows a rather good textural stability (Figs. 1 and 2, see also [12,13]), it is still possible that under high-temperature hydrogen treatment minor variations of grain size and surface roughness occur that are not detectable by profile imaging. The observation by Chojnacki et al. [33] that an increasing mobility of the support with reduction temperature may play a role in ceria supporting *films* led us to

check possible structural changes under reducing conditions on a thin crystalline ceria support (Fig. 3). A ceria film of 20 nm nominal thickness, prepared by high-vacuum deposition on a NaCl support at 573 K and mounted on a gold EM grid, was subjected to reduction in 1 bar hydrogen at increasing temperature. Fig. 3 shows the film after preparation (a) and after reduction at 723 K (b). Since the ceria grains are in part (0 0 1) oriented with respect to the former NaCl support the contrast variations arise mainly from deviation from the Bragg position (Fig. 3a). While the gaps between the single ceria grains start to be filled at about 573 K, substantial coalescence was observed after reduction at 723 K (Fig. 3b), indicating considerable material transport at relatively low temperature. After reduction at 973 K the ceria film is completely closed (not shown here). In agreement with the HREM studies reported in [13] for powder noble metal/CeO₂ catalysts, the observed changes occurring on the ceria film are irreversible upon air exposure, but it cannot be completely excluded that similar mass transport may also lead to partial reversible coverage (decoration) of the metal surface which is removed upon exposure to air.

3.1.3. Interaction of Pt/SiO₂ with hydrogen under high-temperature reduction

Silica-supported noble metals are representative for classical “non-SMSI” behaviour, and in particular the Pt/silica system has been extensively studied in a Europe-wide attempt to standardize experimentally determined catalytic properties [34].

The standard catalyst EUROPT-1 (6% Pt on silica) was already the subject of a previous investigation of MCB ring opening in our group [20], but studies by electron diffraction and lattice-resolved electron microscopy are hampered by its high dispersion. Therefore, we used the Pt (20%)/silica catalyst to exemplify irreversible alterations of supported

noble metal particles on inert supports upon high-temperature reduction. The higher metal loading and the higher atomic number of Pt (compared to Rh) provide a better contrast in the electron microscope.

The behaviour of Pt/silica upon reduction has received some attention in the literature (e.g. [35–39]). Particle shape changes due to hydrogen treatments around 873 K were interpreted as due to anisotropic surface free energy changes of different crystal faces [35,37]. After reduction above 873 K, Pt–Si alloy formation was first suspected [36], and later detected [37,39]. Some of us have shown that reduction of the silica support and formation of Pt–Si alloy can start already upon reduction at 773 K if epitaxially grown Pt particles are (partly) embedded in a silica film [31,39]. Hence, it was of interest to study the behaviour of an impregnated catalyst with metal particles of comparable size on top of the support under identical conditions.

We reduced the Pt/silica catalyst in 1 bar hydrogen at increasing temperature for increasing periods of time. Indeed, formation of Pt–Si alloys could be detected, although a prolonged hydrogen treatment at very high temperature was required. Fig. 4 shows electron micrographs of representative Pt particles as grown (a), and after a hydrogen treatment at 1073 K for 18 h (b). A microdiffraction pattern of a single particle, identified as Pt₁₂Si₅ on [2 1 0] zone axis, is also shown (c), together with a simulated diffraction pattern (d). During the whole treatment the mean Pt particle size has increased from 32 to 42 nm. The corresponding X-ray diffractograms of Fig. 4e indicate that the transition from pure Pt to Pt₁₂Si₅ has occurred at 1073 K. As mentioned above, we had observed formation of Pt₁₂Si₅ and of Si-richer alloys on silica-embedded particles Pt under extended hydrogen treatments already between 773 and 873 K [40]. Most likely, the intimate contact between particles and support favours recrystallization and alloying at much lower temperatures.

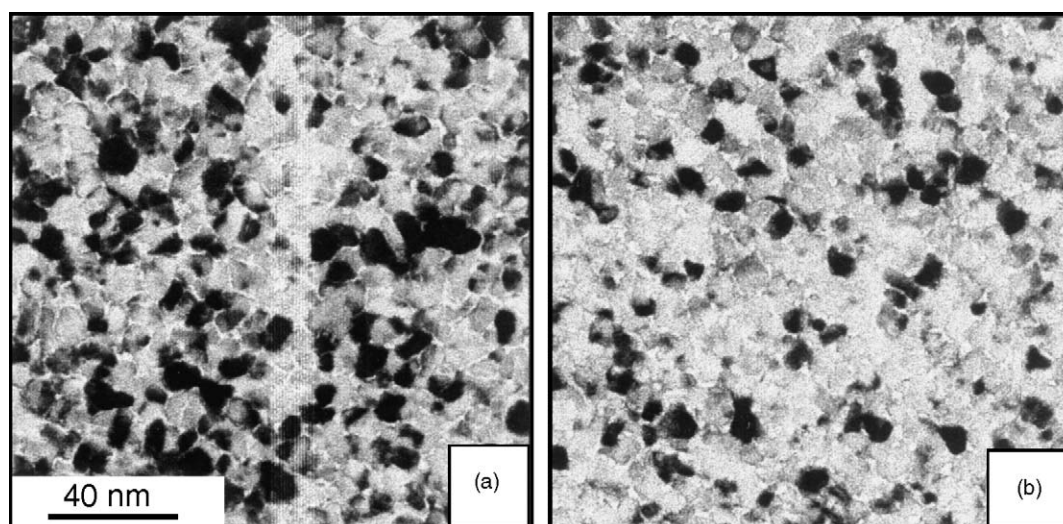


Fig. 3. Ceria film (20 nm mean thickness) deposited on NaCl at 673 K, as grown (a) and after reduction in 1 bar hydrogen at 723 K (b).

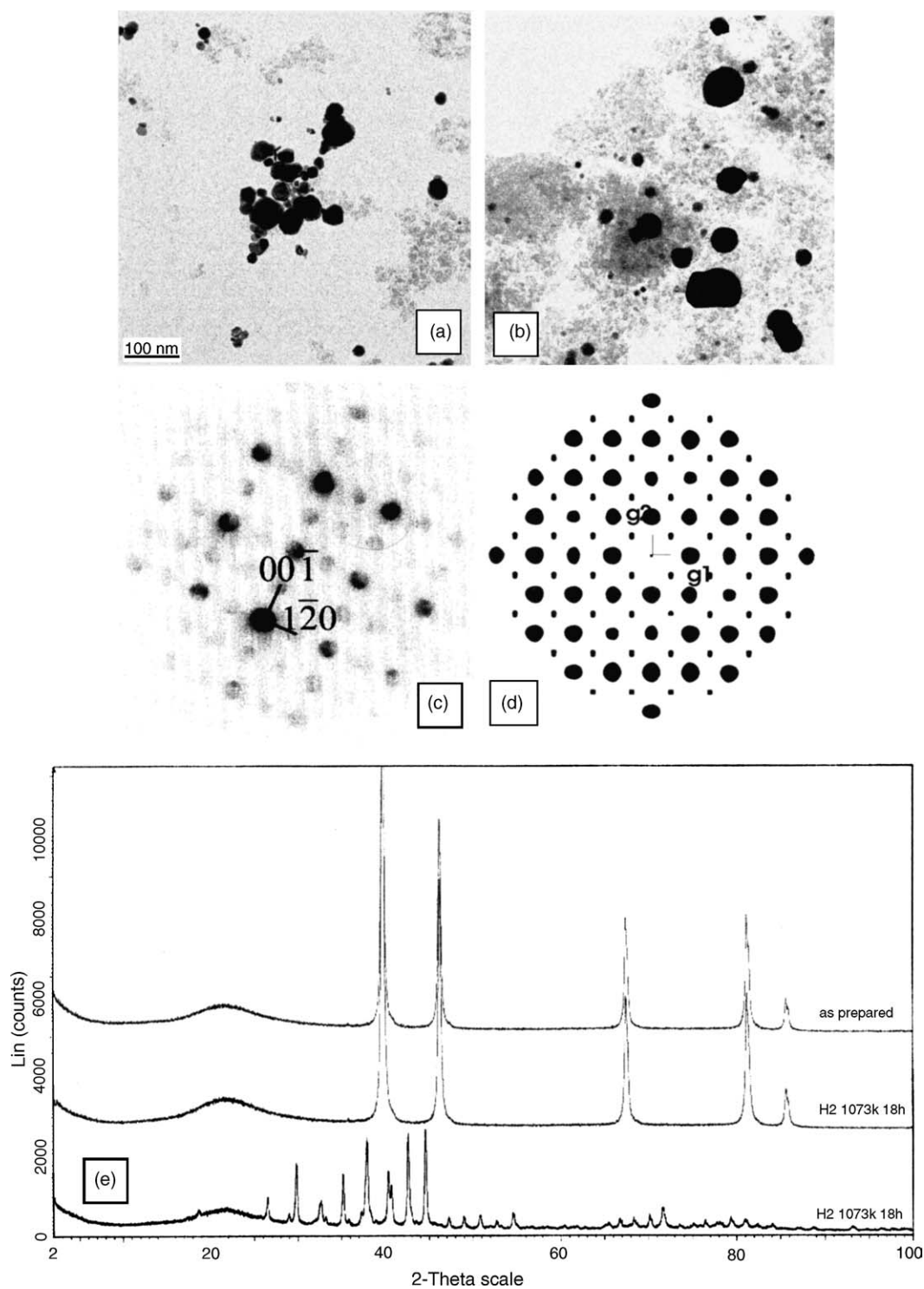


Fig. 4. The Pt (20%)/SiO₂ catalyst calcined and reduced at 673 K (a); and after reduction in 1 bar hydrogen at 1073 K for 18 h (b); microdiffraction pattern of a Pt₁₂Si₅ particle (c); and corresponding simulated diffraction pattern (d); X-ray diffractogram before reduction and after reduction at 873 and 1073 K (e).

3.2. Hydrogenolysis of methylcyclobutane

As mentioned before, the hydrogenolytic ring opening of methylcyclobutane is suited for studying the effect of low- and mid-temperature reduction on skeletal hydrocarbon reactions

since it occurs at 373 K and below. At low temperature and under hydrogen excess only the ring opening products *n*-pentane and isopentane are formed. As discussed above, their proportion on Pt and Rh catalysts is different, but in the present work only the *overall* rates are taken for a comparison.

3.2.1. MCB ring opening on Pt/ceria (Fig. 5)

The catalyst was preoxidized at 673 K for 120 min and reduced at a given temperature for 60 min (standard pretreatment), before the ring opening of methylcyclobutane was followed. After reoxidation at 673 K this procedure was repeated with varying reduction temperature. The highest activity was observed after reduction at 373 K which was also the reaction temperature. After reduction in the low-temperature regime (473–573 K) the activity decreased only slightly, but upon further reduction at 673 and 723 K a significant drop was observed. In Fig. 5 (▲) the initial turnover frequency is plotted versus the reduction temperature. The initial TOF after low-temperature reaction of about 1 h^{-1} is similar to that measured previously for the same reaction on EUROPT-1 (a Pt/SiO₂ catalyst of about 60% dispersion) under identical experimental conditions [20], but one should note that on both catalysts the rates of this reaction are extremely sensitive to hydrogen pressure. A plot of log TOF versus log P_{H_2} yields a reaction order of -0.7 in hydrogen in the range between 10 and 500 mbar. At 10 mbar hydrocarbon and 100 mbar H₂ pressure, the apparent activation energy is 54 kJ/mol, measured between 323 and 473 K. If the catalyst was annealed in vacuum at 723 K for 30 min after every reduction step (Fig. 5 (●)) the activity decreases from 30 to 20% of the value observed immediately after reduction, except after reduction at 723 K where a small activity increase is observed. In general, neither activating nor deactivating treatments had significant effects on the reaction orders or on the apparent energy of activation, if measured under identical reaction conditions. However, as also noted previously, these parameters are strongly sensitive to the hydrogen pressure.

3.2.2. MCB ring opening on Rh/ceria (Fig. 6)

Under comparable reaction conditions the impregnated Rh/ceria catalyst is far more active than its Pt/ceria counterpart, but it shows a similar behaviour upon reduction. At 303 K initial turnovers between 5 and 10 h^{-1} are measured. After preoxidation at 673 K the highest activity is observed if an annealing step in vacuum at 723 K is

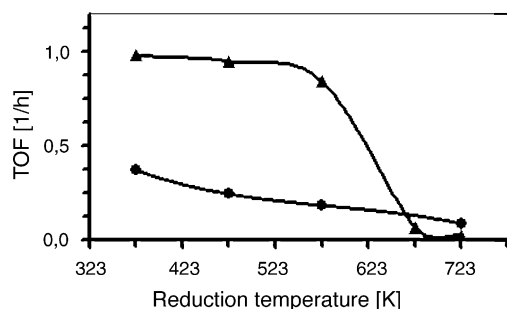


Fig. 5. MCB ring opening on Pt (4%)/CeO₂, initial activity vs. reduction temperature. Pretreatment: (▲) O₂ 673 K (2 h), H₂ 373–723 K (1 h); (●) O₂ 673 K (2 h), H₂ 373–723 K (1 h), followed by annealing in vacuum at 723 K (30 min). Reaction conditions: 10 mbar MCB, 100 mbar H₂, 890 mbar He, 373 K.

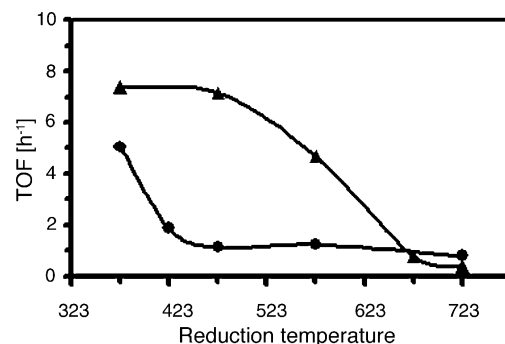


Fig. 6. MCB ring opening on Rh (2.5%)/CeO₂, initial activity vs. reduction temperature. Pretreatment: (▲) O₂ 673 K (2 h), H₂ 373–723 K (1 h); (●) O₂ 673 K (2 h), H₂ 373–723 K (1 h), followed by annealing in vacuum at 723 K (30 min). Reaction conditions: 10 mbar MCB, 100 mbar H₂, 890 mbar He, 303 K.

introduced *before* reduction at 373 K (Fig. 6 (▲)). After the same pretreatment and a following reduction at 473 K the activity is almost unchanged. However, upon further reduction it decreases rapidly and reaches 1/10 of the initial value after reduction at 723 K. In contrast, an annealing step at 723 K *after* the reduction (●) caused a general strong activity decrease, except for the highest reduction temperature.

3.3. Hydrogenation of CO

CO hydrogenation on Pt and Rh is known to be promoted by addition of ceria to an inert support [11,41] which also favours formation of longer chain hydrocarbons and/or alcohols [17]. Compared to MCB hydrogenolysis, it proceeds at a somewhat lower rate and higher reaction temperatures had to be chosen (523 K on Pt and 473 K on Rh). (This higher reaction temperature, of course, limits the temperature range available for studying reduction effects prior to reaction.) Under the given reaction conditions (hydrogen excess about 10:1, reaction temperature $\geq 473 \text{ K}$) the main product is methane ($>90\%$ on Pt/ceria, 80–90% on Rh/silica, 60–80% on Rh/ceria).

3.3.1. CO hydrogenation on Pt/ceria (Fig. 7)

After oxygen treatment (673 K, 2 h) the initial rates were determined at 523 K as a function of hydrogen reduction (1 bar, 1 h) at increasing temperature (reaction mixture 10 mbar CO, 100 mbar H₂ and 890 mbar He). A strong rate decrease with reduction temperature is observed up to 723 K. The rates of CO hydrogenation on Pt/ceria at 523 K (Fig. 7) are comparable to those on Rh/ceria at 473 K (Fig. 8).

It is worth to refer to earlier information about the chemisorptive properties of the Pt/ceria catalyst [12,13]. Pure ceria chemisorbs significant amounts of CO, the amount depending on its redox state [12] and the individual contributions of metal and support to the overall chemisorbed CO cannot be discriminated by volumetric techniques.

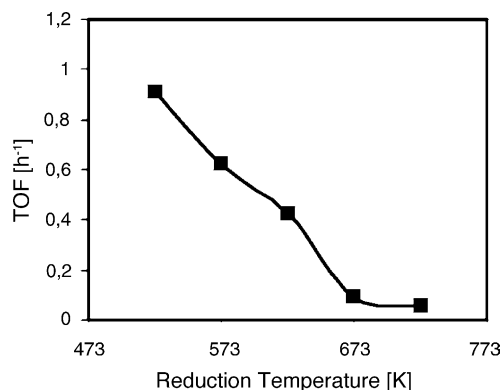


Fig. 7. Rate of CO hydrogenation on Pt (4%)/CeO₂ as a function of reduction temperature. Pretreatment: O₂ 673 K (2 h), H₂ 523–723 K (1 h). Reaction conditions: 10 mbar CO, 100 mbar H₂, 890 mbar He, 523 K.

However, because of the specificity of IR bands due to CO bonded to the metal surface, this limitation is circumvented by FTIR spectroscopy, which has been used to investigate the metal chemisorption capability of a Pt/CeO₂ sample, reduced at increasing temperatures [16]. In this study a progressive inhibition of Pt chemisorption capability for CO was found to occur between 473 and 773 K.

3.3.2. CO hydrogenation on Rh/silica (Fig. 8)

Silica-supported Rh is known for non-SMSI behaviour, at least under low- and medium-temperature reduction. Under the chosen reaction conditions (473 K, 10 mbar CO, 100 mbar hydrogen, 890 mbar He) the initial turnover of CO hydrogenation is about 0.3 h⁻¹, in agreement with the values reported for a pure Rh surface extrapolated to the

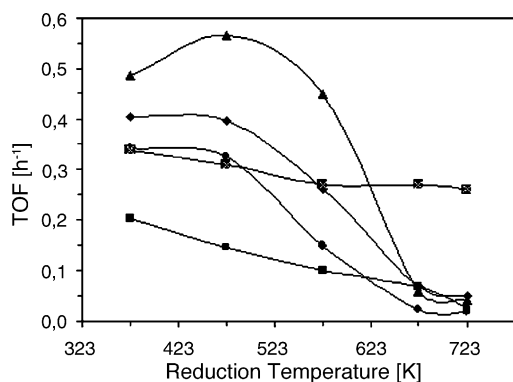


Fig. 8. Initial rate of CO hydrogenation on Rh (3%)/SiO₂ (■) and on Rh (2.5%)/CeO₂ (◆, ▲, ■, ●) as a function of reduction temperature and of different additional treatments. (■) Rh (3%)/SiO₂, O₂ 673 K (2 h), H₂ 373–723 K (1 h); (◆) Rh (2.5%)/CeO₂, O₂ 673 K (2 h), H₂ 373–723 K (1 h); (▲) Rh (2.5%)/CeO₂, O₂ 673 K (2 h), annealing in vacuum 723 K (30 min), H₂ 373–723 K (1 h); (■) Rh (2.5%)/CeO₂, O₂ 673 K (2 h), H₂ 373–723 K (1 h), annealing in vacuum 723 K, (30 min); (●) Rh (2.5%)/CeO₂, O₂ 673 K (2 h), annealing in vacuum 723 K, (30 min), H₂ 373–723 K (1 h), 10 mbar H₂O added to reaction mixture. Reaction conditions: (■, ▲, ◆, ■) 10 mbar CO, 100 mbar H₂, 890 mbar He, 473 K; (●) 10 mbar CO, 100 mbar H₂, 10 mbar H₂O, 880 mbar He.

given reaction conditions [25,42]. Also the measured selectivity towards alkanes (80–90% methane at 473 K) corresponds to that reported for pure rhodium. The reaction orders in hydrogen and CO were determined to be +0.7 and –0.2, respectively, and an Arrhenius plot obtained between 448 and 573 K results in an activation energy of 75 kJ/mol, all that quite independent of oxidative or reductive pretreatments. The low activation energy measured on Rh/silica (75 kJ/mol, compared to 114 kJ/mol on Rh/ceria, see below) may point to a special mechanism of CO activation at lower temperature, as discussed by Demri et al. [43]. In Fig. 8 (■) the overall activity of the Rh/silica catalyst is plotted as a function of reduction temperature in the range between 373 and 723 K (after a foregoing oxygen treatment at 673 K). It is seen that reduction in this temperature range does not have a significant effect on the catalytic activity.

3.3.3. CO hydrogenation on Rh/ceria (Fig. 8)

Contrary to Rh/silica, the hydrogenation of CO on Rh/ceria depends strongly on the reduction temperature. The reactions were again performed at 473 K under standard conditions (10 mbar CO, 100 mbar hydrogen, 890 mbar He). The reaction orders (measured after standard pretreatment) were +0.6 for hydrogen and –0.4 for CO, and the activation energy in the range between 448 and 573 K was 114 kJ/mol. These parameters agree with previously reported data for this reaction on supported Rh catalysts [43].

In Fig. 8 the results of three pretreatments of the Rh/ceria catalyst are presented. In the standard activation (◆) the catalyst was oxidized at 673 K (2 h) and then reduced for 1 h at the stated temperature. The (total) initial activity is shown as a function of T_{red} between 373 and 723 K. After reduction at 373 and 473 K the reaction rate is somewhat higher than on Rh/silica, but it declines after reduction at 573 K, and more strongly at 673 K, before levelling off at 723 K. This behaviour is completely reversible by subsequent oxidation at 673 K, leading to reaction rates reproducible within less than 10%. If an annealing step (723 K in vacuum, 30 min) is introduced before the reduction (▲), the reaction rates are somewhat higher and between reduction at 373 and 473 K (the reaction temperature) even an increase is observed. However, if the catalyst was annealed at 723 K after the reduction step (■) all rates were again significantly decreased.

A previous study of the kinetics of CO hydrogenation on ceria-supported Rh by Trovarelli et al. [18] has resulted in increased turnover rates after reduction in the 773 K range hydrogen under transient conditions. It is reasonable to assume that the different behaviour of Rh/ceria under static and transient conditions arises from the effect of the water formed during reaction, which drives the concurrent water gas shift reaction but is suppressed under transient conditions. In order to assess the effect of water in our batch-like reactor, a substantial amount of water vapour (10 mbar) was added to the reactants and the reactions were

performed after the standard pretreatment under otherwise identical conditions. The results, also presented in Fig. 8 (●), indeed indicate a general shift to lower reaction rates in the presence of water, hence confirming the above assumption.

4. Discussion

The interpretation of the kinetic results is intimately connected to two questions: (i) the reducibility of the support surface and (ii) possible structural changes of the metal particles and/or the support during reductive treatments at low and medium temperature.

4.1. Reducibility of ceria

Ceria reduction leading to Ce^{3+} species has long been considered responsible for the decreased activity in some hydrocarbon reactions after reduction in hydrogen [14]. Under reducing conditions the ceria support consists of CeO_{2-x} , x being the fraction of oxygen vacancies in the bulk or at the surface. The vacancies are compensated by an equivalent number of Ce^{3+} ions in the lattice. Upon reduction or annealing in vacuum the number of oxygen vacancies and Ce^{3+} ions increases. In particular, reduction between 473 and 673 K results in a strong increment of vacancies and Ce^{3+} ions on the surface (30–60%, [39,40]), while their transport into the bulk becomes significant at 673 K above [14]. It seems therefore that both reactions are favoured by a rather oxidized state of the ceria support (which is not necessarily the same for hydrocarbon activation and CO hydrogenation) and that the activity decreases with the further increasing number of Ce^{3+} ions on the surface. Concerning CO hydrogenation, previous studies have shown that ceria may enhance the activity of Pt and Rh, either as a support or as an additive to an inert support [17,18,44,45], whereby the extent of enhancement depends on the actual ceria loading and on the reduction temperature. As mentioned above, Trovarelli et al. [18] observed a rate increase under transient conditions after reduction at 773 K while in the steady state the reaction rate was rather low compared to after LTR. The different behaviour of Rh/ceria under static and transient conditions arises most likely from the influence of the water formed during reaction on the concurrent water gas shift reaction. In our experiments a negative influence of water on the reaction rate could definitely be stated.

In all experiments the main rate decline occurs in the same range of reduction temperatures (>573–673 K). Additional annealing steps at 723 K before reduction improve the activity whereas annealing after reduction has a stronger negative influence on the rates than the reduction itself (except for reduction at 723 K). These two effects are not easily quantified but clearly connected to the onset of bulk diffusion of oxygen at the respective

temperature since annealing at 573 K shows almost no effect.

Recent studies dealing with thin ceria overlayers on Rh [46,47] and Pt [48,49] single crystal surfaces have allowed some insight into the stoichiometry and microstructure of the metal–ceria boundary. These systems, also denoted as “inverse” supported catalysts, were studied under UHV-compatible conditions by scanning tunnelling microscopy (STM) and photoelectron spectroscopy (XPS). Reducing conditions, including heating in vacuum, induce the formation of Ce^{III} species at the immediate interface between a Rh(1 1 1) surface and the overlaying oxide, and an enhanced mobility of thin ceria overlayers at elevated temperature (673 K), leading increased decoration of the noble metal surface [47]. These changes observed on ceria overlayers were found to be reversible as Ce^{3+} is easily reoxidized on the surface under atmospheric conditions. Some of us studied the kinetics of CO hydrogenation on a polycrystalline Rh surface covered with submonolayers of ceria [25], and observed that submonolayers of ceria favour the reaction after low-temperature reduction while higher reduction temperature induces a rate decline apparently related to increasing Ce^{3+} formation. The extrapolation of the kinetic results obtained on impregnated, thin film and inverse model catalysts to equivalent experimental conditions, using the experimentally determined reaction orders and activation energies, showed a good agreement of the turnover rates on these three types of catalyst.

4.2. Structural changes

Regarding the effect of reduction temperature on the structure of dispersed metal nanoparticles, a number of factors must be considered. As already mentioned, changes in the morphology of the metal nanocrystals, particularly of rhodium, are likely to occur (see below). In addition, other phenomena such as metal decoration and Ce–noble metal alloying should be taken into account [13]. Another effect, i.e. support sintering with inherent metal encapsulation [12], is unlikely because of the low surface area and the high textural stability of the ceria support, and of the moderate reduction temperatures (≤ 723 K). In fact, no modification of the BET surface area could be observed upon reduction at the above mentioned temperatures. Likewise, as deduced from the metal dispersion reported in the experimental section, metal sintering effects are rather moderate and therefore excluded as a significant factor causing the observed catalyst deactivations.

On Pt/ceria and Rh/ceria the rates of both MCB hydrogenolysis and CO hydrogenation decrease strongly in the range around 673 K. However, the different evolution with T_{red} of the activity of Pt and Rh deserves some comments. On Pt/ CeO_2 , the MCB activity decreases sharply for $T_{\text{red}} > 573$ K whereas on Rh/ CeO_2 , the deactivation effects are already noticeable at lower T_{red} , and very significant at $T_{\text{red}} = 573$ K. This observation contrasts with

earlier results on hydrogen chemisorption [12,13], according to which the sensitivity to deactivation induced by increasing reduction temperatures would be higher on Pt/CeO₂ than on Rh/CeO₂. Because of the structure-sensitive nature of the reaction, this disagreement suggests the simultaneous occurrence of different deactivation mechanisms. Also a recent study of structure-insensitive hydrocarbon reactions on Pt/CeO₂ and Rh/CeO₂ [50] suggests that electronic effects are more important for reductive deactivation of Pt than of Rh.

Modifications in the morphology of the metal particles, in addition to the onset of metal/support interaction effects, might cooperate to the observed activity loss. The former contribution is probably more relevant on rhodium catalysts, because, as already stressed, the oxygen pretreatment routine applied here before any activity run ensures the full reoxidation of Rh nanoparticles [51,23] to Rh₂O₃. Accordingly, on rhodium the subsequent reduction treatment must induce deeper structural changes than on platinum, for which reoxidation only affects the outer layers of the metal nanocrystals. To summarize, at the lowest reduction temperatures, 373 and 473 K, the high activity of Rh/CeO₂ may result from the formation of metal particles poorly crystallized and, consequently, with a high content of structural defects [51,52,23]. If so, the loss of activity observed upon reduction at 573 K will reflect the formation, as revealed by a number of HREM studies [12,51], of well faceted rhodium nanocrystals, an effect that may be superimposed with the onset of metal-support interaction. Likewise, the effects of annealing before and after reduction on the activity of Rh particles are most likely due to changes of their morphology and size distribution. Annealing of oxidized catalysts at 723 K *before* reduction results in more extended Rh₂O₃ phases which in turn are converted to Rh particles of different microstructure and defect concentration after subsequent low-temperature reduction [51,23]. By contrast, annealing *after* reduction improves the crystallinity of both Rh and Pt particles and removes defects arising from LTR, resulting in a less active catalyst for a structure-sensitive reaction.

It should also be mentioned that reduction of the ceria surface may induce structural defects (step edges) acting as possible anchoring sites for noble metal particles (cf. Fig. 2b). With further increasing reduction temperature, the transition of the support from the semiconducting to the metallic state will lead to increasing loss of electronic site isolation.

Finally, the possibility of alloying, or the early stages thereof, must be discussed. From the thermodynamic viewpoint formation of Pt–Ce and Rh–Ce alloys at and below 773 K at 1 bar hydrogen pressure is feasible (provided minimized water pressure), which means that their generation is only kinetically hindered. Some previous authors have either observed or concluded alloying between the noble metal and cerium around 773 K [33,53], but considerable differences have been reported for Pt–Ce

and Rh–Ce alloying processes suggesting either a different kinetic behaviour or subtle differences in the preparation conditions, particularly in the actual water vapour pressure under which the reduction occurs. Some of us have previously investigated the changes in structure and morphology of ceria-supported epitaxially grown Pt particles subjected to various reduction procedures between 673 and 1073 K, and compared them to “non-SMSI” systems (Pt/silica and Pt/alumina) treated under identical conditions [40,54]. There we observed that alloy formation in Pt/ceria may start already under reduction at 723–773 K if the conditions allow a toptactic growth of similarly structured regular particles, e.g. Pt₃Ce. However, within this range of reduction temperature, ex situ HREM studies of conventional supported catalysts [11–13] have not provided evidence of the formation of well-defined intermetallic Ce–noble metal compounds. Impregnated Pt/ceria catalysts require reduction temperatures well above 1000 K to induce the formation of a Pt₅Ce intermetallic phase [11–13]. The above results are not necessarily contradicting, being obtained under quite different experimental conditions. Obviously, an intimate contact between metal particles and ceria support, connected with increased nucleation probability at the respective interface, favours alloy growth at much lower temperatures than previously experienced. On the other hand, the described behaviour of “non-reducible” inert supports like silica (Fig. 4 versus [40]), and alumina [54] shows clearly that the conditions for alloy formation are obviously much less favourable on impregnated than on thin film catalysts. This means that alloying does most likely not contribute to the observed activity decrease in our Pt/CeO₂ catalyst.

On powder Rh/CeO₂ samples, as in the present study, no evidence of Ce–Rh alloying phenomena could be deduced from HREM studies, even on catalysts reduced at 1173 K. However, the formation of intermetallic phases with crystallographic characteristics that prevent their identification by electron microscopy and diffraction cannot be completely ruled out [52]. The detection of defined Rh–Ce alloy phases in thin film model systems is less straightforward than that of Pt₃Ce [54] because the former are not formed in a single composition or in defined shapes. For completeness, we mention that penetration of Rh metal in the ceria bulk has also been discussed as possible explanation for some phenomena observed after HTR [55]. However, the HREM studies carried out on powder samples [12,13] render the occurrence of a burial effect rather unlikely.

5. Summary and conclusions

The progressive loss of activity observed for both methylcyclobutane hydrogenolysis and CO hydrogenation on low surface area ceria-supported Pt and Rh catalysts upon reduction below 723 K is most likely due to electronic

perturbations at the interface between the metal nanocrystals and the increasingly reduced ceria support. Additional factors like reversible metal decoration or alloying phenomena may not be completely excluded because of the ex situ nature of the current HREM studies. However, since HREM was able to unambiguously detect even monolayer decorations as well as Pt–Ce intermetallic phases [13] on the same catalysts (after reduction at much higher temperatures) the probability of these alternative interpretations is rather low. Purely electronic effects have already been considered as the most likely phenomena involved in the reversible loss of chemisorption capability in Pt/CeO₂ and Pt/CeZrO₂ catalysts reduced at temperatures similar to those applied here [13]. Moreover, FTIR studies of CO chemisorbed on Pt/CeO₂ have revealed that a partial recovery of the catalyst reduced at 773 K could be achieved by very mild reoxidation treatments with CO₂ at 473 K [16]. The regeneration from decorated or alloyed states in noble metal/CeO₂ catalysts would require more severe oxidation conditions, i.e. reoxidation temperatures up to 973 K [13].

In the case of Rh/CeO₂ it is likely that changes in the morphology of the rhodium crystallites with increasing T_{red} will also contribute to the observed deactivation. This would explain the observed sensitivity of Rh/CeO₂ to the reduction temperature. The reduction of ceria-supported oxidized Rh particles (Rh₂O₃) at the lowest temperatures, 373–473 K, may lead to highly defective metal particles with enhanced activity towards a structure-sensitive reaction such as MCB hydrogenolysis.

Acknowledgements

This work was supported by the Austrian Science Fund (Project S 8105), by the Austrian–Spanish research cooperation Acciones Integradas (Project 4/2002), and by the Spanish MCYT (Project MAT2002-02782).

References

- [1] S.J. Tauster, S.C. Fung, R.L. Garten, *J. Am. Chem. Soc.* 100 (1978) 170; G.L. Haller, D.E. Resasco, *Adv. Catal.* 36 (1989) 173.
- [2] A.K. Singh, N.K. Pande, A.T. Bell, *J. Catal.* 94 (1985) 422.
- [3] E. Braunschweig, A.D. Logan, A.K. Datye, D.J. Smith, *J. Catal.* 118 (1989) 227.
- [4] F. Pesty, H.P. Steinrück, T.E. Madey, *Surf. Sci.* 339 (1995) 83.
- [5] A. Berkó, J. Ulrych, K.C. Prince, *J. Phys. Chem. B* 102 (1998) 3379.
- [6] J.P. Belzunegui, J. Sanz, J.M. Rojo, *J. Am. Chem. Soc.* 112 (1990) 4066.
- [7] S. Bernal, J.J. Calvino, M.A. Cauqui, G.A. Cifredo, A. Jobacho, J.M. Rodríguez-Izquierdo, *Appl. Catal. A* 99 (1993) 1.
- [8] S. Penner, D. Wang, R. Schlögl, K. Hayek, *Thin Solid Films* 484 (2005) 10.
- [9] S. Bernal, J. Botana, J.J. Calvino, C. López, J.A. Pérez-Omil, J.M. Rodríguez-Izquierdo, *J. Chem. Soc., Faraday Trans.* 92 (1996) 2799.
- [10] S. Bernal, F.J. Botana, J.J. Calvino, G.A. Cifredo, J.A. Pérez-Omil, J.M. Pintado, *Catal. Today* 23 (1995) 219.
- [11] S. Bernal, J.J. Calvino, J.M. Gatica, C. Larese, C. López-Cartes, J.A. Pérez-Omil, *J. Catal.* 169 (1997) 510.
- [12] S. Bernal, J.J. Calvino, M.A. Cauqui, J.M. Gatica, C. Larese, J.A. Pérez-Omil, J.M. Pintado, *Catal. Today* 50 (1999) 175.
- [13] S. Bernal, J.J. Calvino, J.M. Gatica, C. Larese, C. López-Cartes, J.M. Pintado, in: A. Trovarelli (Ed.), *Catalysis by Ceria and Related Materials*, Imperial College Press, London, 2002, p. 85.
- [14] A. Trovarelli, *Catal. Rev.-Sci. Eng.* 38 (1996) 439.
- [15] G. Rupprechter, M. Fuchs, K. Hayek, J.A. Pérez-Omil, C. López-Cartes, J.J. Calvino, S. Bernal, *Stud. Surf. Sci. Catal.* 140 (2000) 2021.
- [16] S. Bernal, G. Blanco, J.M. Gatica, C. Larese, H. Vidal, *J. Catal.* 200 (2001) 411.
- [17] M.A. Vannice, *J. Catal.* 37 (1975) 449.
- [18] A. Trovarelli, G. Dolcetti, C. de Leitenburg, J. Kaspar, P. Finetti, A. Santoni, *J. Chem. Soc., Faraday Trans.* 88 (1992) 1311; A. Trovarelli, G. Dolcetti, C. de Leitenburg, J. Kaspar, *Stud. Surf. Sci. Catal.* 75 (1993) 2781.
- [19] G. Maire, G. Plouidy, J.C. Prudhomme, F.C. Gault, *J. Catal.* 4 (1965) 556.
- [20] C. Zimmermann, K. Hayek, *New frontiers in catalysis*, in: L. Guzzi, et al. (Eds.), *Proceedings of the 10th International Congress on Catalysis Budapest 1992*, Elsevier, Amsterdam, 1993, p. 2375.
- [21] B. Török, M. Bartók, *Catal. Lett.* 27 (1994) 281.
- [22] B. Török, M. Török, M. Bartók, *Catal. Lett.* 33 (1995) 321.
- [23] G. Rupprechter, G. Seeber, H. Goller, K. Hayek, *J. Catal.* 186 (1999) 201.
- [24] Z. Paál, M. Dobrovolszky, *React. Kinet. Catal.* 1 (1974) 435.
- [25] B. Jenewein, M. Fuchs, K. Hayek, *Surf. Sci.* 532–535 (2003) 364.
- [26] S. Penner, D. Wang, R. Podloucky, R. Schlögl, K. Hayek, *Phys. Chem. Chem. Phys.* 6 (2004) 1.
- [27] J. Cunningham, D. Cullinane, J. Sanz, J.M. Rojo, X.A. Soria, J.L.G. Fierro, *J. Chem. Soc., Faraday Trans.* 88 (1992) 3233.
- [28] S. Bernal, J.J. Calvino, G.A. Cifredo, J.M. Rodríguez-Izquierdo, *J. Phys. Chem.* 99 (1995) 11794.
- [29] C. Force, J.P. Belzunegui, J. Sanz, A. Martínez-Arias, J. Soria, *J. Catal.* 197 (2001) 192.
- [30] S. Bernal, G. Blanco, J.J. Calvino, M.A. Cauqui, J.M. Rodríguez-Izquierdo, H. Vidal, *J. Alloys Compd.* 250 (1997) 461.
- [31] S. Penner, D. Wang, D.S. Su, G. Rupprechter, R. Podloucky, R. Schlögl, K. Hayek, *Surf. Sci.* 532–535 (2003) 276.
- [32] C. Zimmermann, K. Hayek, *Chem. Ing. Tech.* 63 (1991) 68.
- [33] T. Chojnacki, K. Krause, L.D. Schmidt, *J. Catal.* 128 (1991) 161.
- [34] G.C. Bond, F. Garin, G. Maire, *Appl. Catal.* 41 (1988) 313.
- [35] A.D. van Langeveld, B.E. Nieuwenhuys, V. Ponc, *Thin Solid Films* 105 (1983) 9.
- [36] T. Wang, C. Lee, L.D. Schmidt, *Surf. Sci.* 163 (1985) 181.
- [37] R. Lamber, N. Jaeger, *J. Appl. Phys.* 70 (1991) 457.
- [38] A.S. Ramachandran, S.L. Anderson, A.K. Datye, *Ultramicroscopy* 51 (1993) 282.
- [39] W. Juszczyk, D. Lomot, J. Pielaszek, Z. Karpinski, *Catal. Lett.* 78 (2002) 95.
- [40] D. Wang, S. Penner, D.S. Su, G. Rupprechter, K. Hayek, R. Schlögl, *J. Catal.* 219 (2003) 434.
- [41] J.R. Katzer, A.W. Sleight, P. Gajardo, J. Michel, E.F. Gleason, S. McMillan, *Faraday Disc. Chem. Soc.* 72 (1981) 121.
- [42] W. Reichl, K. Hayek, *J. Catal.* 208 (2002) 422.
- [43] D. Demri, J.P. Hindermann, A. Kiennemann, C. Mazzocchia, *Catal. Lett.* 23 (1994) 227.
- [44] P. Meriaudeau, M. Dufaux, C. Naccache, *ACS Symposium Series* 298 (Strong Metal-Support Interaction), vol. 298, 1986, p. 118.
- [45] D. Kalakkad, A.K. Datye, H. Robota, *Appl. Catal. B* 1 (1992) 191.
- [46] D.R. Mullins, S.H. Overbury, D.R. Huntley, *Surf. Sci.* 409 (1998) 307.
- [47] S. Eck, C. Castellarin-Cudía, S. Surnev, K.C. Prince, M.G. Ramsey, F.P. Netzer, *Surf. Sci.* 536 (2003) 166.
- [48] C. Hardacre, G.M. Roe, R.M. Lambert, *Surf. Sci.* 326 (1995) 1.

- [49] K.D. Schierbaum, Surf. Sci. 399 (1998) 29.
- [50] D. Teschner, A. Wootsch, K. Matusek, T. Röder, Z. Paál, Solid State Ionics 141 (2001) 709.
- [51] G. Rupprechter, K. Hayek, H. Hofmeister, J. Catal. 173 (1998) 409.
- [52] A.D. Logan, K.S. Sharoudi, A.K. Datye, J. Phys. Chem. 95 (1991) 5568.
- [53] S. Penner, D. Wang, R. Podloucky, R. Schlögl, K. Hayek, Phys. Chem. Chem. Phys. 6 (2004) 1.
- [54] S. Penner, G. Rupprechter, H. Sauer, D.S. Su, R. Tessadri, R. Podloucky, R. Schlögl, K. Hayek, Vacuum 71 (2003) 71.
- [55] S. Imamura, T. Yamashita, R. Hamada, Y. Saito, Y. Nakao, N. Tsuda, C. Kaito, J. Mol. Catal. A 128 (1998) 249.